Exploring $B \to \omega\mu^+\mu^-$ decay with Z' boson

M. Mandal[*] and S. Sahoo[†]

Department of Physics, National Institute of Technology Durgapur Durgapur-713209, West Bengal, India

(Received 23 February 2026; accepted 29 April 2026; published 2 June 2026)

Rare decays of B mesons play a crucial role in understanding and exploring the intricacies of physics beyond the standard model. Various experimental results as well as theoretical investigations involving rare B meson decays have motivated us to investigate the rare decay, $B \to \omega\mu^+\mu^-$, proceeding through the quark transition $b \to d\ell^+\ell^-$ in standard model and nonuniversal Z' model. We have incorporated the new physics (NP) couplings of the Z' boson with quarks from $B_d - \overline{B_d}$ mixing. We have estimated the NP leptonic couplings from the experimental values of branching fractions of other $b \to d\ell^+\ell^-$ decays. With these NP couplings, we have estimated the branching ratio, forward-backward asymmetry, and lepton polarization asymmetries. We have observed significant deviation from standard model predictions, especially for the branching fraction and forward-backward asymmetry.

DOI: 10.1103/brtr-td9f

I. INTRODUCTION

The B meson decay sector provides excellent opportunities to explore possible new physics (NP) signatures and introduces plenty of prospects to examine interactions beyond the present framework of the standard model (SM). Recent experimental and phenomenological scenarios depict a growing interest in the investigations involving flavour changing neutral current (FCNC) decays. In the SM, these transitions arise through the Glashow-Iliopoulos-Maiani amplitudes at loop level [1,2]. Furthermore, the involvement of the weak mixing angles of the Cabibbo-Kobayashi-Maskawa (CKM) matrix also suppresses these decays [2–4], thus increasing their sensitivity to potential NP contributions.

Several experimental observations in the B meson decay sector which involve $b \to s\ell^+\ell^-$ transition have prompted many theoretical and phenomenological searches for NP. For example, the SM results [5] show tensions of 4.2σ for $B^+ \to K^+\mu^+\mu^-$ [6] and 3.1σ for $B^0 \to K^0\mu^+\mu^-$ (in $1.1 < q^2 < 6\ \mathrm{GeV}^2$) [6]. In the high $q^2 (15 < q^2 < 22\ \mathrm{GeV}^2)$ region, too, there has been a tension of 2.7σ between SM results and LHCb results for $B^0 \to K^0\mu^+\mu^-$ [6]. For $B_s^0 \to \phi\mu^+\mu^-$ decay, there is a deviation of 3.6σ of the branching ratio, from the SM predictions, for the region $1.1 < q^2 < 6\ \mathrm{GeV}^2$ [7]. Furthermore, the LHCb observed a local discrepancy of 3.7σ in the range of $4.30 < q^2 < 8.68\ \mathrm{GeV}^2$ for the angular observable P_5' for the decay $B^0 \to K^*(892)^0\mu^+\mu^-$ [8]. Also, for the integrated value of P_5' over the interval $1.0 < q^2 < 6.0\ \mathrm{GeV}^2$, the discrepancy is 2.5σ with SM estimations [8]. Global analysis performed with the CP-averaged observables indicate deviation of 3.4σ from the SM in the case of the $B^0 \to K^{*0}\mu^+\mu^-$ decay mode [9].

As the $b \to d\ell^+\ell^-$ decays can be complementary probes to the $b \to s\ell^+\ell^-$ channels, we can likewise scrutinize potential hints of NP in the $b \to d\ell^+\ell^-$ decays. In fact, the branching fractions of $b \to d\ell^+\ell^-$ decays are further suppressed by a factor of $|\frac{V_{td}}{V_{ts}}|^2 \simeq 0.04$, which makes them even more influenced by NP than the $b \to s$ counterparts [10]. Moreover, the $b \to d\ell^+\ell^-$ decays are susceptible to the CP-violating phase β as they are sensitive to the CKM matrix element V_{td}. Contrary to this, $b \to s\ell^+\ell^-$ decays depict sensitivity to V_{ts}, and the corresponding CP phase is $\beta_s \approx 0$. Consequently, comparatively higher CP-violating effects can be anticipated for the case of $b \to d\ell^+\ell^-$ decays [11].

Considering the potential of $b \to d\ell^+\ell^-$ transitions to provide stringent tests of SM and discover possible NP signatures, these transitions have been explored extensively in several phenomenological studies [11–22]. For formulating NP, one can take either of two approaches: one involves adding new symmetries to SM for framing NP models, and the other is where new massive fields are incorporated using generic effective field theory [23]. Models such as the Z' model, the W' model, and the leptoquark model introduce particles which are not present in the SM. These theoretical frameworks with NP particles have been utilized in several phenomenological studies of $b \to d$ transition. In the nonuniversal Z' model, the decays $B \to \rho\ell^+\ell^-$ and $B \to \pi\ell^+\ell^-$, which occur through $b \to d$ transition, have been investigated with the estimation of various observables including the differential branching ratio, CP-violation asymmetry, and lepton polarization asymmetry [12]. The influence of the Z' boson on several important observables including different

[*]Contact author: manosheemandal@gmail.com
[†]Contact author: sukadevsahoo@yahoo.com

angular observables has also been explored for the decay mode $B \to (\rho, a_1)\mu^+\mu^-$ [13]. In Ref. [14], a global fit with $b \to s\ell^+\ell^-$ and $b \to d\ell^+\ell^-$ observables has been performed to constrain NP couplings of the Z' boson and study their effects on $B_s \to \overline{K}^*\ell^+\ell^-$. Other than the Z' model, $B \to \rho\ell^+\ell^-$ and $B \to \pi\ell^+\ell^-$ decays have also been examined in the two Higgs doublet model with focus on branching ratio, CP violation, and forward-backward asymmetry [15]. Furthermore, model-independent analysis for the decay, $B_s \to K^*(\to K\pi)\mu^+\mu^-$ has depicted deviations from SM predictions for several observables [16]. Model-independent analysis has also been performed from global fits to $B_s^0 \to \bar{K}^{*0}\mu^+\mu^-$, $B^+ \to \pi^+\mu^+\mu^-$, $B^0 \to \mu^+\mu^-$, and $B \to X_d\gamma$ decays [17]. A number of $b \to d\ell^+\ell^-$ decays like $B \to \pi\ell^+\ell^-$, $B \to \rho\ell^+\ell^-$, and $B \to \omega\ell^+\ell^-$ are recently examined in the theory of the covariant confined quark model as well [18].

Although $b \to d$ decays have immense potential to provide pathways for exploring NP, their typical branching fractions in the SM, which are calculated to be of the order of $\mathcal{O}(10^{-8})$ [24–26], or even smaller than this, makes them difficult to observe in experiments [10]. Nevertheless, in 2012, the LHCb observed and measured the branching fraction of $B^+ \to \pi^+\mu^+\mu^-$ decay as $(2.3 \pm 0.6(\mathrm{stat}) \pm 0.1(\mathrm{syst})) \times 10^{-8}$ [27]. This [27] is considered to be the first ever measurement for a $b \to d$ transition. Later on, the LHCb Collaboration also measured the CP asymmetry for the same decay [28]. The *BABAR* Collaboration has set branching fraction upper limits on $B^0 \to \eta\ell^+\ell^-$ and $B^0 \to \pi^0\ell^+\ell^-$ decays [29]. LHCb has also measured the branching fractions of $B^0 \to \pi^+\pi^-\mu^+\mu^-$ and $B^0 \to \rho^0\mu^+\mu^-$ to be $(2.11 \pm 0.51(\mathrm{stat}) \pm 0.15(\mathrm{syst})) \times 10^{-8}$ and $(1.98 \pm 0.53) \times 10^{-8}$, respectively [30]. A recent experimental study using a 711 fb^{-1} data sample carried out by the Belle Collaboration has performed searches for several $b \to d\ell^+\ell^-$ decays, such as $B^{+,0} \to (\eta, \omega, \pi^{+,0}, \rho^{+,0})\ell^+\ell^-$ [10]. These experimental investigations motivate us to explore further and perform phenomenological analysis on $b - d\ell^+\ell^-$ transition.

In the present work, in order to investigate NP, we have explored $B \to \omega\mu^+\mu^-$ decays as a promising probe for possibilities of NP signatures in the $b \to d\ell^+\ell^-$ sector. The upper limit on the branching fraction of this decay has recently been set by the Belle Collaboration [10]. This decay has also been previously analyzed in the covariant confined quark model [18]. In our work, we perform a detailed phenomenological analysis of this decay and evaluate various observables such as the branching fraction, forward-backward asymmetry, and lepton polarization asymmetry in the nonuniversal Z' model and compare the results with the corresponding SM predictions. We have constrained the NP quark couplings from $B_d - \bar{B}_d$ mixing. To obtain the NP leptonic couplings of the Z' boson, we have performed a χ^2 fit with experimental results of branching fractions of the decays which proceed through $b \to d$ transition. We have used the available experimental results for $B^+ \to \pi^+\mu^+\mu^-$, $B_s^0 \to K^{*0}\mu^+\mu^-$, and $B^0 \to \rho^0\mu^+\mu^-$ decays in our χ^2 fit.

In the following section, we discuss the theoretical framework required for formulating the expressions of the observables of $b \to d\mu^+\mu^-$ transition. In Sec. III, we describe the framework and NP couplings in the nonuniversal Z' model. We describe how we estimated the NP couplings and modified the Wilson coefficients in Sec. IV. We then discuss the results obtained in Sec. V.

II. $b \to d\mu^+\mu^-$ TRANSITION IN SM

A. Effective Hamiltonian and Wilson coefficients

In the SM, the $b \to d\mu^+\mu^-$ transition is described through an effective Hamiltonian, in terms of operator product expansion. The effective Hamiltonian may be written as [18,24,31–33]

$$H_{\mathrm{eff}}^{\mathrm{SM}} = -\frac{4G_F}{\sqrt{2}} V_{td}^* V_{tb} \left\{ \sum_{i=1}^{10} C_i(\mu) O_i(\mu) + \lambda_u \sum_{i=1}^{2} C_i(\mu) [O_i(\mu) - O_i^{(u)}(\mu)] \right\}. \tag{1}$$

In this basis, the short-distance physics is encoded in the Wilson coefficients C_i. The local operators $O_{1,2}$ represent the current-current operators, O_{3-6} correspond to QCD penguin operators, the dipole operators are represented by $O_{7,8}$, and the semileptonic electroweak penguin operators are denoted by $O_{9,10}$ [18]. These local operators, in terms of chirality projection operators $P_{L,R} = (1 \mp \gamma_5)/2$, can be written as [18,32,33]

$$\begin{aligned}
O_1^u &= (\bar{d}_{a_1}\gamma^\mu P_L u_{a_2})(\bar{u}_{a_2}\gamma_\mu P_L b_{a_1}), \qquad O_2^u = (\bar{d}\gamma^\mu P_L u)(\bar{u}\gamma_\mu P_L b), \\
O_1 &= (\bar{d}_{a_1}\gamma^\mu P_L c_{a_2})(\bar{c}_{a_2}\gamma_\mu P_L b_{a_1}), \qquad O_2 = (\bar{d}\gamma^\mu P_L c)(\bar{c}\gamma_\mu P_L b), \\
O_3 &= (\bar{d}\gamma^\mu P_L b)\Sigma_q(\bar{q}\gamma_\mu P_L q), \qquad O_4 = (\bar{d}_{a_1}\gamma^\mu P_L b_{a_2})\Sigma_q(\bar{q}_{a_2}\gamma_\mu P_L q_{a_1}),
\end{aligned}$$

$$O_5 = (\bar{d}\gamma^\mu P_L b)\Sigma_q(\bar{q}\gamma_\mu P_R q), \qquad O_6 = (\bar{d}_{a_1}\gamma^\mu P_L b_{a_2})\Sigma_q(\bar{q}_{a_2}\gamma_\mu P_R q_{a_1}),$$
$$O_7 = \frac{e^2}{16\pi^2}\bar{m}_b(\bar{d}\sigma^{\mu\nu}P_R b)F_{\mu\nu}, \qquad O_8 = \frac{g}{16\pi^2}\bar{m}_b(\bar{d}_{a_1}\sigma^{\mu\nu}P_R \mathbf{T}_{a_1a_2}b_{a_2})\mathbf{G}_{\mu\nu},$$
$$O_9 = \frac{e^2}{16\pi^2}(\bar{d}\gamma^\mu P_L b)(\bar{l}\gamma_\mu l), \qquad O_{10} = \frac{e^2}{16\pi^2}(\bar{d}\gamma^\mu P_L b)(\bar{l}\gamma_\mu\gamma_5 l).$$

The dipole operator O_7 is represented in terms of photon field strength $F_{\mu\nu}$, while O_8 is constructed with the gluon field strength $\mathbf{G}_{\mu\nu}$ and the $SU(3)$ color group generators $\mathbf{T}_{a_1a_2}$. The renormalization scale is represented by μ [18].

The matrix element is written as [2,18,31,32]

$$\mathscr{M}(b \to d\ell^+\ell^-) = \frac{G_F\alpha}{\sqrt{2}\pi}V_{td}^*V_{tb}\left\{C_9^{\rm eff}[\bar{d}\gamma_\mu P_L b][\bar{\ell}\gamma^\mu\ell] + C_{10}[\bar{d}\gamma_\mu P_L b][\bar{\ell}\gamma^\mu\gamma_5\ell] - 2\hat{m}_b C_7^{\rm eff}\left[\bar{d}i\sigma_{\mu\nu}\frac{\hat{q}^\nu}{\hat{s}}P_R b\right][\bar{\ell}\gamma^\mu\ell]\right\}. \quad (2)$$

We have followed the approach of Ref. [2] and denote the $\overline{\rm MS}$ (Modified Minimal Subtraction) mass evaluated at a scale μ as $m_b \equiv m_b(\mu)$ and the pole mass of the $b-$ quark as $m_{b,\rm pole}$. In perturbation theory, up to next-to-leading order, these two masses are related by [2]

$$m_b(\mu) = m_{b,\rm pole}\left[1 - \frac{4}{3}\frac{\alpha_s(\mu)}{\pi}\left\{1 - \frac{3}{4}\ln\left(\frac{m_{b,\rm pole}^2}{\mu^2}\right)\right\}\right]. \quad (3)$$

We choose $\mu_b = \sqrt{M_B^2 - m_b^2} \simeq 2.4$ GeV as the scale of the B decays. The values of the Wilson coefficients considered in our work are given in Table I. The effective Wilson coefficient $C_9^{\rm eff}$ is written as [31,34,35]

$$\begin{aligned} C_9^{\rm eff}(\hat{s}) = {} & C_9 + g(\hat{m}_c,\hat{s})[3C_1 + C_2 + 3C_3 + C_4 + 3C_5 + C_6] \\ & - \frac{1}{2}g(1,\hat{s})[4C_3 + 4C_4 + 3C_5 + C_6] - \frac{1}{2}g(0,\hat{s})[C_3 + 3C_4] \\ & + \frac{2}{9}[3C_3 + C_4 + 3C_5 + C_6] - \frac{V_{ud}^*V_{ub}}{V_{td}^*V_{tb}}[3C_1 + C_2][g(0,\hat{s}) - g(\hat{m}_c,\hat{s})], \end{aligned} \quad (4)$$

with

$$g(0,\hat{s}) = \frac{8}{27} - \frac{8}{9}\ln\frac{m_b}{\mu} - \frac{4}{9}\ln\hat{s} + \frac{4}{9}i\pi, \quad (5)$$

$$\begin{aligned} g(z,\hat{s}) = {} & \frac{8}{27} - \frac{8}{9}\ln\frac{m_b}{\mu} - \frac{8}{9}\ln z + \frac{4}{9}x - \frac{2}{9}(2+x)\sqrt{|1-x|} \\ & \times \begin{cases} \left(\ln\left|\frac{\sqrt{1-x}+1}{\sqrt{1-x}-1}\right| - i\pi\right) & \text{for } x \equiv \frac{4z^2}{\hat{s}} \le 1, \\ 2\arctan\frac{1}{\sqrt{x-1}} & \text{for } x \equiv \frac{4z^2}{\hat{s}} > 1. \end{cases} \end{aligned} \quad (6)$$

B. Form factors

The transition matrix elements required for describing the above decays may be classified into semileptonic and penguin contributions [34,36–38]. The penguin type form factors can be described in terms of the semileptonic type form factors as [34]

TABLE I. Wilson coefficients [34].

C_1	C_2	C_3	C_4	C_5	C_6	$C_7^{\rm eff}$	C_9	C_{10}
−0.360	1.169	0.017	−0.036	0.010	−0.048	−0.355	4.42	−4.398

$$T_1(q^2) = \frac{M_B^2 - M_\omega^2 + q^2}{2M_B}\frac{V(q^2)}{M_B + M_\omega} + \frac{M_B + M_\omega}{2M_B}A_1(q^2), \tag{7}$$

$$T_2(q^2) = \frac{2}{M_B^2 - M_\omega^2}\left[\frac{(M_B - y)(M_B + M_\omega)}{2}A_1(q^2) + \frac{M_B(y^2 - M_\omega^2)}{M_B + M_\omega}V(q^2)\right], \tag{8}$$

$$T_3(q^2) = -\frac{M_B + M_\omega}{2M_B}A_1(q^2) + \frac{M_B - M_\omega}{2M_B}[A_2(q^2) - A_3(q^2)] + \frac{M_B^2 + 3M_\omega^2 - q^2}{2M_B(M_B + M_\omega)}V(q^2), \tag{9}$$

with $y = \frac{M_B^2 + M_\omega^2 - q^2}{2M_B}$ being the energy of the final light meson.

Four independent form factors, A_1, A_2, A_3, and V, are required for the $B \to \omega$ decay mode. In this study, we have used these form factors obtained from light cone sum rules [34]. We utilize the following parametrization to obtain reasonable behavior of the form factors since at large momentum transfer ($q^2 \sim m_Q^2$) light cone sum rules break down [34],

$$F(q^2) = \frac{F(0)}{1 - a_F\frac{q^2}{M_B^2} + b_F\left(\frac{q^2}{M_B^2}\right)^2}, \tag{10}$$

where $F(q^2)$ denotes the form factors A_i and V.

The form factors for $B \to \omega$ decay used in our study are given in Table II.

C. Expressions of observables

Following the approach of Refs. [2,34,39,40], the decay width can be constructed in terms of auxiliary coefficients, and these auxiliary coefficients are in turn structured in terms of form factors and Wilson coefficients. Thus, the decay width can be described as

$$\frac{d\Gamma}{d\hat{s}} = \frac{G_F^2\alpha^2 M_B^5}{2^{10}\pi^5}|V_{td}^* V_{tb}|^2\hat{u}(\hat{s})D, \tag{11}$$

where

$$\begin{aligned} D = {} & \frac{|A|^2}{3}\hat{s}\lambda\left(1 + 2\frac{\hat{m}_\mu^2}{\hat{s}}\right) + |E|^2\hat{s}\frac{\hat{u}(\hat{s})^2}{3} \\ & + \frac{1}{4\hat{M}_\omega^2}\left[|B|^2\left(\lambda - \frac{\hat{u}(\hat{s})^2}{3} + 8\hat{M}_\omega^2(\hat{s} + 2\hat{m}_\mu^2)\right) + |F|^2\left(\lambda - \frac{\hat{u}(\hat{s})^2}{3} + 8\hat{M}_\omega^2(\hat{s} - 4\hat{m}_\mu^2)\right)\right] \\ & + \frac{\lambda}{4\hat{M}_\omega^2}\left[|C|^2\left(\lambda - \frac{\hat{u}(\hat{s})^2}{3}\right) + |G|^2\left(\lambda - \frac{\hat{u}(\hat{s})^2}{3} + 4\hat{m}_\mu^2(2 + 2\hat{M}_\omega^2 - \hat{s})\right)\right] \\ & - \frac{1}{2\hat{M}_\omega^2}\left[\mathrm{Re}(BC^*)\left(\lambda - \frac{\hat{u}(\hat{s})^2}{3}\right)(1 - \hat{M}_\omega^2 - \hat{s}) + \mathrm{Re}(FG^*)\left(\left(\lambda - \frac{\hat{u}(\hat{s})^2}{3}\right)(1 - \hat{M}_\omega^2 - \hat{s}) + 4\hat{m}_\mu^2\lambda\right)\right] \\ & - 2\frac{\hat{m}_\mu^2}{\hat{M}_\omega^2}\lambda[\mathrm{Re}(FH^*) - \mathrm{Re}(GH^*)(1 - \hat{M}_\omega^2)] + \frac{\hat{m}_\mu^2}{\hat{M}_\omega^2}\hat{s}\lambda|H|^2 \end{aligned} \tag{12}$$

with $\hat{m}_\mu = m_\mu/M_B$, and $\hat{M}_\omega = M_\omega/M_B$.

TABLE II. Form factors [34].

	$F(0)$	a_F	b_F
A_1	$0.221^{+0.012}_{-0.013}$	$0.46^{-0.01}_{+0.02}$	$-0.08^{-0.01}_{+0.01}$
A_2	$0.211^{+0.011}_{-0.011}$	$1.16^{-0.01}_{+0.01}$	$0.35^{-0.01}_{+0.01}$
A_3	$-0.211^{+0.011}_{-0.011}$	$1.16^{+0.01}_{-0.01}$	$0.35^{+0.01}_{-0.01}$
V	$0.275^{+0.014}_{-0.015}$	$1.40^{-0.02}_{+0.02}$	$0.51^{-0.02}_{+0.04}$

The auxiliary functions are represented by A, B, C, E, F, G, and H, and they are structured as [2]

$$A(\hat{s}) = \frac{2}{1+\hat{M}_\omega} C_9^{\text{eff}}(\hat{s}) V(\hat{s}) + \frac{4\hat{m}_b}{\hat{s}} C_7^{\text{eff}} T_1(\hat{s}), \tag{13}$$

$$B(\hat{s}) = (1+\hat{M}_\omega)\left[C_9^{\text{eff}}(\hat{s}) A_1(\hat{s}) + \frac{2\hat{m}_b}{\hat{s}}(1-\hat{M}_\omega) C_7^{\text{eff}} T_2(\hat{s})\right], \tag{14}$$

$$C(\hat{s}) = \frac{1}{1-\hat{M}_\omega^2}\left[(1-\hat{M}_\omega) C_9^{\text{eff}}(\hat{s}) A_2(\hat{s}) + 2\hat{m}_b C_7^{\text{eff}}\left(T_3(\hat{s}) + \frac{1-\hat{M}_\omega^2}{\hat{s}} T_2(\hat{s})\right)\right], \tag{15}$$

$$E(\hat{s}) = \frac{2}{1+\hat{M}_\omega} C_{10} V(\hat{s}), \tag{16}$$

$$F(\hat{s}) = (1+\hat{M}_\omega) C_{10} A_1(\hat{s}), \tag{17}$$

$$G(\hat{s}) = \frac{1}{1+\hat{M}_\omega} C_{10} A_2(\hat{s}), \tag{18}$$

$$H(\hat{s}) = \frac{1}{1+\hat{M}_\omega} C_{10} A_3(\hat{s}). \tag{19}$$

The terms $\lambda(\hat{s})$ and $\hat{u}(\hat{s})$ are

$$\lambda(\hat{s}) = 1 + \hat{M}_\omega^4 + \hat{s}^2 - 2\hat{s} - 2\hat{M}_\omega^2(1+\hat{s}), \tag{20}$$

$$\hat{u}(\hat{s}) = \sqrt{\lambda(\hat{s})\left(1 - 4\frac{\hat{m}_\mu^2}{\hat{s}}\right)}. \tag{21}$$

The forward-backward asymmetry is expressed as [2]

$$\begin{aligned} \frac{d\mathcal{A}_{FB}}{d\hat{s}} &= \frac{G_F^2 \alpha^2 M_B^5}{2^{10}\pi^5} |V_{td}^* V_{tb}|^2 \hat{s}\, \hat{u}\,(\hat{s})^2 [\text{Re}(BE^*) + \text{Re}(AF^*)] \\ &= \frac{G_F^2 \alpha^2 M_B^5}{2^8 \pi^5} |V_{td}^* V_{tb}|^2 \hat{s}\, \hat{u}\,(\hat{s})^2 C_{10} [\text{Re}(C_9^{\text{eff}}) V A_1 \\ &\quad + \frac{\hat{m}_b}{\hat{s}} C_7^{\text{eff}} \{V T_2 (1-\hat{M}_\omega^2) + A_1 T_1 (1+\hat{M}_\omega)\}]. \end{aligned} \tag{22}$$

In the plot of forward-backward asymmetry, we need to equate the two parts of the expressions in the square brackets of Eq. (22) [2]. Thus, at the zero-crossing point,

$$\text{Re}(C_9^{\text{eff}}(\hat{s}_0)) = -\frac{\hat{m}_b}{\hat{s}_0} C_7^{\text{eff}} \left\{\frac{T_2(\hat{s}_0)}{A_1(\hat{s}_0)}(1-\hat{M}_\omega) + \frac{T_1(\hat{s}_0)}{V(\hat{s}_0)}(1+\hat{M}_\omega)\right\}. \tag{23}$$

From the experimental perspective, the normalized forward-backward asymmetry is more advantageous, and it is defined as [2]

$$\frac{d\bar{\mathcal{A}}_{FB}}{d\hat{s}} = \frac{d\mathcal{A}_{FB}}{d\hat{s}} \Big/ \frac{d\Gamma}{d\hat{s}}. \tag{24}$$

In terms of lepton polarization asymmetries [40],

$$\frac{d\Gamma(\hat{u})}{d\hat{s}} = \frac{1}{2}\left(\frac{d\Gamma}{d\hat{s}}\right)_0 [1 + (P_L \hat{e}_L + P_N \hat{e}_N + P_T \hat{e}_T).\hat{n}], \tag{25}$$

where $(\frac{d\Gamma}{d\hat{s}})_0$ is the unpolarized decay width and $\hat{n}$ represents unit vector in the center of mass frame of dilepton. P_L, P_N, and P_T represent longitudinal polarization asymmetry, normal polarization asymmetry, and transverse polarization asymmetry, respectively. Both P_L and P_T are in the decay plane, while P_N is perpendicular to the decay plane.

Following Refs. [39,40], we write the lepton polarization asymmetry P_i as

$$P_i(\hat{s}) = \frac{\frac{d\Gamma(\hat{n}=\hat{e}_i)}{d\hat{s}} - \frac{d\Gamma(\hat{n}=-\hat{e}_i)}{d\hat{s}}}{\frac{d\Gamma(\hat{n}=\hat{e}_i)}{d\hat{s}} + \frac{d\Gamma(\hat{n}=-\hat{e}_i)}{d\hat{s}}}, \tag{26}$$

$$P_L D = \sqrt{1-4\frac{\hat{m}_\mu^2}{\hat{s}}}\left\{\frac{2\hat{s}\lambda}{3}\text{Re}(AE^*) + \frac{(\lambda + 12\hat{s}\hat{M}_\omega^2)}{3\hat{M}_\omega^2}\text{Re}(BF^*) - \frac{\lambda(1-\hat{M}_\omega^2-\hat{s})}{3\hat{M}_\omega^2}\text{Re}(BG^* + CF^*) + \frac{\lambda^2}{3\hat{M}_\omega^2}\text{Re}(CG^*)\right\}, \tag{27}$$

$$P_N D = \frac{-\pi\sqrt{\hat{s}}\hat{u}(\hat{s})}{4\hat{M}_\omega}\left\{\frac{\hat{m}_\mu}{\hat{M}_\omega}[\text{Im}(FG^*)(1+3\hat{M}_\omega^2-\hat{s}) + \text{Im}(FH^*)(1-\hat{M}_\omega^2-\hat{s}) - \text{Im}(GH^*)\lambda] + 2\hat{M}_\omega \hat{m}_\mu [\text{Im}(BE^*) + \text{Im}(AF^*)]\right\}, \tag{28}$$

$$P_T D = \frac{\pi\sqrt{\lambda}\hat{m}_\mu}{4\sqrt{\hat{s}}}\left\{4\hat{s}\mathrm{Re}(AB^*) + \frac{(1-\hat{M}_\omega^2-\hat{s})}{\hat{M}_\omega^2}[-\mathrm{Re}(BF^*) + (1-\hat{M}_\omega^2)\mathrm{Re}(BG^*) + \hat{s}\mathrm{Re}(BH^*)]\right.$$
$$\left. + \frac{\lambda}{\hat{M}_\omega^2}[\mathrm{Re}(CF^*) - (1-\hat{M}_\omega^2)\mathrm{Re}(CG^*) - \hat{s}\mathrm{Re}(CH^*)]\right\}. \qquad (29)$$

With the expressions of these observables and the form factors, we estimate their values for $B \to \omega\mu^+\mu^-$ decays.

III. Z' MODEL

The Z' boson is a hypothetical beyond-the-standard-model particle and is a colorless, chargeless vector boson. The Z' boson is introduced in several theoretical models such as grand unified theories, supersymmetric extensions of SM, theories with large extra dimensions, and superstring theories [41–49]. In family nonuniversal Z' models, flavor mixing in the quark and lepton sectors leads to flavor-changing couplings of the Z' boson [41]. Because of the nondiagonal chiral coupling matrix, the FCNC transitions occur at the tree level in the nonuniversal Z' model [22]. Models with flavor nonuniversal Z' couplings have been extensively used in phenomenological studies of FCNC decays [12–14,22,39,50–55].

In the Z' model, the $U(1)'$ currents may be expressed as [12,41,56,57]

$$J_\mu = \sum_{i,j}\bar{\psi}_i\gamma_\mu[\epsilon_{\psi_{L_{ij}}}P_L + \epsilon_{\psi_{R_{ij}}}P_R]\psi_j, \qquad (30)$$

where $\epsilon_{\psi_{R,L_{ij}}}$ represent the chiral couplings of the Z' boson. It is considered that the Z' couplings are diagonal and nonuniversal [12]. Thus, fermion mixing induces flavor-changing couplings. These FCNCs occur at tree level in the Z' model in both the left-handed and the right-handed sectors. We write the couplings explicitly as [12]

$$B_{ij}^{\psi_L} \equiv (V_L^\psi \epsilon_{\psi_L} V_L^{\psi^\dagger})_{ij}, \quad B_{ij}^{\psi_R} \equiv (V_R^\psi \epsilon_{\psi_R} V_R^{\psi^\dagger})_{ij}. \qquad (31)$$

Neglecting $Z - Z'$ mixing and considering that only the right-handed quark couplings with the Z' boson are diagonal [12,58–66], the modified Hamiltonian for the Z' part is written as [12]

$$H_{\mathrm{eff}}^{Z'} = \frac{2G_F}{\sqrt{2}\pi}V_{tb}V_{td}^*\left[\frac{B_{db}^L B_{\ell\ell}^L}{V_{tb}V_{td}^*}\bar{d}\gamma_\mu(1-\gamma_5)b\bar{\ell}\gamma^\mu(1-\gamma_5)\ell\right.$$
$$\left. + \frac{B_{db}^L B_{\ell\ell}^R}{V_{tb}V_{td}^*}\bar{d}\gamma_\mu(1-\gamma_5)b\bar{\ell}\gamma^\mu(1+\gamma_5)\ell\right], \qquad (32)$$

where $B_{db}^L = |B_{db}^L|e^{-i\phi_{db}^L}$ denotes the off-diagonal left-handed couplings of quark sector with the Z' boson and ϕ_{db}^L is the new weak phase. Thus,

$$H_{\mathrm{eff}}^{Z'} = -\frac{4G_F}{\sqrt{2}}V_{tb}V_{td}^*[C_9^{Z'}O_9 + C_{10}^{Z'}O_{10}], \qquad (33)$$

with [12]

$$C_9^{Z'} = \frac{4\pi e^{-i\phi_{db}^L}}{\alpha V_{tb}V_{td}^*}|B_{db}^L|(B_{\ell\ell}^L + B_{\ell\ell}^R), \qquad (34)$$

$$C_{10}^{Z'} = \frac{4\pi e^{-i\phi_{db}^L}}{\alpha V_{tb}V_{td}^*}|B_{db}^L|(B_{\ell\ell}^L - B_{\ell\ell}^R). \qquad (35)$$

$B_{\ell\ell}^L$ and $B_{\ell\ell}^R$ represent the couplings of Z' boson with the left- and right-handed leptons, respectively.

Thus, the modified Wilson coefficients, C_9 and C_{10}, including the contributions from both the SM and Z' model, can be written as

$$C_9^{NP} = C_9^{\mathrm{eff}} + C_9^{Z'}, \qquad (36)$$

$$C_{10}^{NP} = C_{10} + C_{10}^{Z'}. \qquad (37)$$

IV. ESTIMATION OF NP COUPLINGS

To investigate the influence of the Z' boson, we need to incorporate NP couplings in the Wilson coefficients C_9 and C_{10}. It has been found in Ref. [67] that the strength of the quark coupling with the Z' boson is strongly constrained by $B_d - \overline{B_d}$ mixing. In Ref. [22], the fitting results of the mixing parameters C_{B_d} and ϕ_{B_d} from the UTfit Collaboration are considered [68,69] for the estimation of the quark coupling. Following Refs. [22,67], we have constrained the available parameter space of NP quark coupling B_{db}^L with the recent results of C_{B_d} and ϕ_{B_d} from the UTfit Collaboration [70].

Here, we discuss the theoretical formulation required for $\bar{B}_d - B_d$ mixing. In the SM, the effective Hamiltonian for $\bar{B}_d - B_d$ mixing is given by [33,67,71,72]

$$\mathscr{H}_{\mathrm{eff}}^{\mathrm{SM}}(\Delta B = 2) = \frac{G_F^2}{16\pi^2}M_W^2(V_{tb}V_{td}^*)^2 \times C_Q(\mu_b)Q(\Delta B = 2) + \mathrm{H.c.}, \qquad (38)$$

where $Q(\Delta B = 2) = (\bar{q}b)_{V-A}(\bar{q}b)_{V-A}$. The off-diagonal term M_{12}^{SM} in the B meson mass matrix is given by [67]

$$2M_{B_d}M_{12}^{\mathrm{SM}} = \langle B_d^0|\mathscr{H}_{\mathrm{eff}}^{\mathrm{SM}}(\Delta B=2)|\bar{B}_d^0\rangle = \frac{G_F^2}{6\pi^2}M_W^2(V_{tb}V_{td}^*)^2(\hat{B}_{B_d}f_{B_d}^2)M_{B_d}^2\eta_B S_0(x_t). \quad (39)$$

Here, M_W denotes the mass of W boson, $\hat{B}_{B_d}$ is the bag parameter, f_{B_d} is the B meson decay constant, η_B is the short-distance QCD correction function, and $S_0(x_t)$ is the Inami-Lim function. For our work, we have taken the values $\eta_B = 0.55$ [33,71] and $f_{B_d}\sqrt{B_{B_d}} = 210.6$ MeV [73]. The Inami-Lim function is given by [71]

$$S_0(x_t) = \frac{4x_t - 11x_t^2 + x_t^3}{4(1-x_t)^2} - \frac{3x_t^3\ln x_t}{2(1-x_t)^3}, \quad (40)$$

where $x_t = (\frac{\bar{m}_t(\bar{m}_t)}{M_W})^2$. We have taken the scale-dependent mass $\bar{m}_t(\bar{m}_t)$ as $m_t^{\overline{\mathrm{MS}}}(m_t) = 162.69$ GeV [74].

Now, in the Z' model, in terms of the NP quark coupling B_{db}^L and the new weak phase ϕ_{db}^L, the contribution of the Z' boson to M_{12} can be written as [67]

$$2M_{B_d}M_{12}^{Z'} = \frac{G_F}{\sqrt{2}}U'_{LL}|B_{db}^L|^2 e^{i2\phi_{db}^L}\frac{8}{3}M_{B_d}^2(\hat{B}_{B_d}f_{B_d}^2), \quad (41)$$

with

$$U'_{LL} = (\alpha_s(\mu_W))^{\frac{\gamma_Q^{(0)}}{2\beta_0}}\left[1 - \frac{\alpha_s(\mu_W)}{4\pi}J_5\right], \quad (42)$$

where $\gamma_Q^{(0)} = 4$ [67,71], $\beta_0 = 23/3$ [67,71], and $J_5 = 1.627$ [67,71].

The UTfit Collaboration has performed model-independent analysis of $\bar{B}_q - B_q$ mixing with the parametrization [68,69]

$$C_{B_q}e^{2i\phi_{B_q}} = \frac{\langle B_q|\mathscr{H}_{\mathrm{eff}}^{\mathrm{full}}|\bar{B}_q\rangle}{\langle B_q|\mathscr{H}_{\mathrm{eff}}^{\mathrm{SM}}|\bar{B}_q\rangle} = \frac{A_q^{\mathrm{SM}}e^{i\phi_q^{\mathrm{SM}}} + A_q^{NP}e^{i(2\phi_q^{NP}+\phi_q^{\mathrm{SM}})}}{A_q^{\mathrm{SM}}e^{i\phi_q^{\mathrm{SM}}}}, \quad (43)$$

where $\mathscr{H}_{\mathrm{eff}}^{\mathrm{full}}$ is the effective Hamiltonian with both SM and NP contributions while $\mathscr{H}_{\mathrm{eff}}^{\mathrm{SM}}$ has only the SM contributions [67]. In the SM, the modulus of C_{B_q} is predicted to be 1, while the phase ϕ_{B_q} is 0 [67]. However, the fit results by the UTfit Collaboration deviate from the SM predictions. Following the methodology of Refs. [22,67], we have estimated the parameter space of the NP quark couplings of the Z' boson, while considering the recent results of the UTfit Collaboration for $\bar{B}_d - B_d$ mixing (Table III). With these data from Table III, the obtained parameter space for the quark coupling B_{db}^L and the new weak phase ϕ_{db}^L is shown in Fig. 1. The overlapping area is the region of allowed coupling. We have performed naïve χ^2 minimization to obtain the values of the quark coupling and the new weak phase. Here, we have defined the χ^2 function as

$$\chi^2 = \sum_i \frac{(\mathcal{O}_i^{th(Z')} - \mathcal{O}_i^{UTfit})^2}{(\Delta\mathcal{O}_i)^2}, \quad (44)$$

where $\mathcal{O}_i^{th(Z')}$'s are the expressions for the parameters C_{B_d} and ϕ_{B_d} including the contribution of Z' boson and $\mathcal{O}_i^{UT\mathrm{fit}}$ is the data from UTfit Collaboration with the uncertainties included in $\Delta\mathcal{O}_i$. The quark coupling B_{db}^L and the new weak phase ϕ_{db}^L obtained by χ^2 minimization are given in Table IV.

To evaluate the leptonic couplings, we have considered the experimental results of branching fractions of the decays $B^+ \to \pi^+\mu^+\mu^-$, $B_s^0 \to K^{*0}\mu^+\mu^-$ and $B^0 \to \rho^0\mu^+\mu^-$

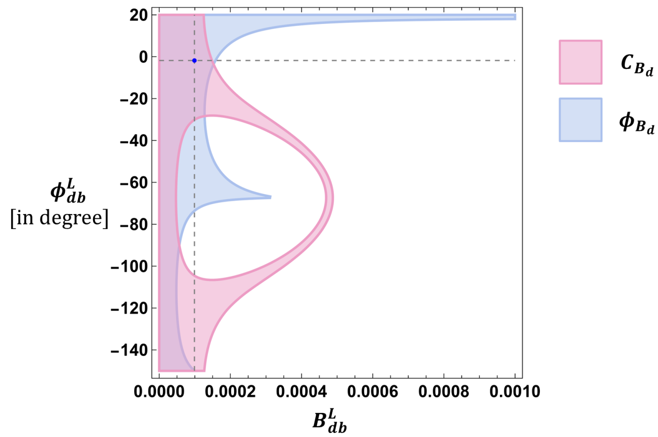

FIG. 1. The quark coupling B_{db}^L and the new weak phase ϕ_{db}^L parameter space constrained from the fit results of the parameters C_{B_d} and ϕ_{B_d} from UTfit Collaboration. The pink region is constrained from C_{B_d}, while the blue region is constrained from ϕ_{B_d}. The overlapping region shows the available parameter space for B_{db}^L and ϕ_{db}^L. The coupling determined by χ^2 minimization is shown by the blue dot.

TABLE III. Fit results from UTfit Collaboration for $\bar{B}_d - B_d$ mixing [70].

Parameter	Value
C_{B_d}	1.06 ± 0.08
$\phi_{B_d}[^\circ]$	-1.8 ± 2.4

TABLE IV. Values of quark coupling and new weak phase.

Parameter	Value
B_{db}^L	0.990×10^{-4}
ϕ_{db}^L	-1.797°

TABLE V. Experimental values of branching ratios of $b \to d\ell^+\ell^-$ decays.

Decay mode	Experimental value
$B^+ \to \pi^+\mu^+\mu^-$	$(1.78 \pm 0.23) \times 10^{-8}$ [74]
$B_s^0 \to K^{*0}\mu^+\mu^-$	$(2.9 \pm 1.1) \times 10^{-8}$ [74]
$B^0 \to \rho^0\mu^+\mu^-$	$(1.98 \pm 0.53) \times 10^{-8}$ [30]

(Table V). The available parameter space of the leptonic couplings $B^L_{\mu\mu}$ and $B^R_{\mu\mu}$ for each decay mode is constrained from the experimental error ranges as well as 1σ theoretical uncertainties. The overlapping space of all the decays gives the allowed region of the leptonic couplings. The 1σ- favored parameter space constrained from $b \to d\ell^+\ell^-$ decays is depicted in Fig. 2. We have also performed a naive χ^2 analysis to obtain the values of the coupling from the allowed parameter space. We have defined χ^2 as [55]

$$\chi^2 = \sum_i \frac{(\mathcal{O}_i^{th}(C_{9,10}^{NP}) - \mathcal{O}_i^{\exp})^2}{(\Delta\mathcal{O}_i^{\exp})^2 + (\Delta\mathcal{O}_i^{\rm SM})^2}, \tag{45}$$

with $\mathcal{O}_i^{th}(C_{9,10}^{NP})$ being the theoretical expressions which include the NP contributions from Z' boson and $\mathcal{O}_i^{\exp}$ being the experimental values of the branching fractions. $\Delta\mathcal{O}_i^{\exp}$ and $\Delta\mathcal{O}_i^{\rm SM}$ represent the 1σ uncertainties of experimental values and theoretically calculated values, respectively. The values of the leptonic couplings obtained by minimizing the χ^2 function is shown by a blue dot in Fig. 2 and also listed in Table VI.

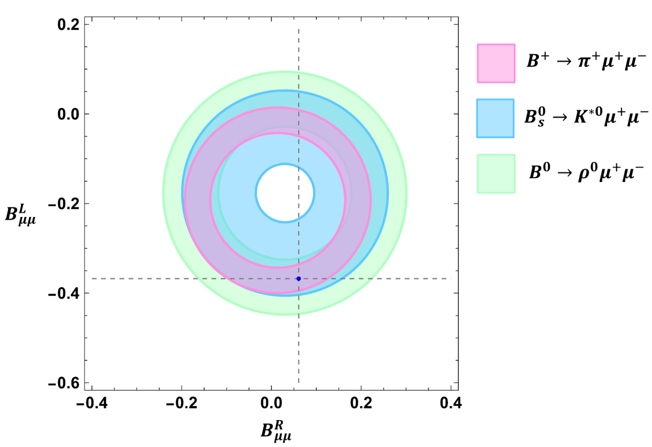

FIG. 2. The leptonic coupling $B^R_{\mu\mu} - B^L_{\mu\mu}$ parameter space constrained from the experimental results of branching fractions of $b \to d\ell^+\ell^-$ decays. The overlapping region shows the available parameter space for the leptonic couplings. The coupling determined by χ^2 minimization is shown by the blue dot.

TABLE VI. Values of leptonic coupling constrained from $b \to d\ell^+\ell^-$ decays.

Left-handed leptonic coupling $B^L_{\mu\mu}$	Right-handed leptonic coupling $B^R_{\mu\mu}$
0.061	−0.368

V. RESULTS OF DIFFERENT OBSERVABLES

With the NP couplings obtained, we have modified the Wilson coefficients C_9 and C_{10}. Incorporating these NP couplings, we have estimated several important observables. We have compared them with the corresponding values in the SM.

The central curves in all the observables, for both the SM and Z' model, have been obtained by considering only the central value of the form factors and other input parameters. The light pink and light blue shaded regions depict the 1σ uncertainties in SM and Z' model, respectively. The uncertainties arise due to the uncertainties of the form factors. We have obtained the 1σ band by varying the form factors within their error ranges.

We have integrated all the observables in the full-$\hat{s}$ range, and the values are given in Table VII. The masses and the decay rates are taken from Ref. [74]. We have listed these values in Table IX of the Appendix. Also, we have considered the CKM matrix coefficients from the SM fit results available at the UTfit website [75]. Following Ref. [18], we have also calculated the observables in two bins in the low-q^2 region, one in $[0.1 - 0.98]$ GeV^2 and the other in $[1.1 - 6]$ GeV^2, while excluding the region of charm resonances. These two bins correspond to [0.003, 0.035] and [0.039, 0.215] in terms of $\hat{s}$ in our study. These results are listed in Table VIII.

The variation of the differential branching ratio with respect to $\hat{s} = q^2/M_B^2$ is shown in Fig. 3(a). In the low-$\hat{s}$ region, the differential branching ratio values are higher in the Z' model compared to the SM values. This enhancement depicts significant influence of the effect of Z' boson. In the mid-$\hat{s}$ region, although there is slight overlap between 1σ uncertainty regions of SM and Z' values, the central values are still higher in the Z' model. However, in the high-$\hat{s}$ region, the differential branching ratio values in the Z' model cannot be distinguished as the 1σ uncertainty region in the Z' model overlaps with that of the SM values. The integrated value of branching ratio over the whole kinematic region is $2.48^{+0.30}_{-0.29} \times 10^{-8}$, while in the Z' model, it is $2.78^{+0.29}_{-0.28} \times 10^{-8}$, which is higher than the SM prediction. Recently, the Belle Collaboration has set the upper limit of the branching fraction for this decay at 24.9×10^{-8} [10]. Our result is within the range of the experimental upper limit.

Figure 3(b) shows how the forward-backward asymmetry varies in the whole dynamical range of momentum

TABLE VII. Integrated values of the observables.

Observable	SM	Z' model
Branching ratio	$2.48^{+0.30}_{-0.29} \times 10^{-8}$	$2.78^{+0.29}_{-0.28} \times 10^{-8}$
Forward-backward asymmetry	$-0.242^{+0.018}_{-0.015}$	$-0.305^{+0.019}_{-0.016}$
Longitudinal lepton polarization asymmetry P_L	$-0.903^{+0.004}_{-0.005}$	$-0.872^{+0.001}_{-0.001}$
Normal lepton polarization asymmetry P_N	$1.937^{+0.117}_{-0.136} \times 10^{-4}$	$2.007^{+0.105}_{-0.101} \times 10^{-3}$
Transverse lepton polarization asymmetry P_T	$5.792^{+0.227}_{-0.307} \times 10^{-2}$	$6.078^{+0.142}_{-0.205} \times 10^{-2}$

transfer squared. In the Z' model, the zero-crossing point vanishes, which is in stark contrast with the SM result. It can be inferred from Eq. (23) that to obtain a zero-crossing point it is required that $\mathrm{sign}(C_7^{\mathrm{eff}} Re(C_9^{\mathrm{eff}})) = -1$ [2]. In the SM, $C_7^{\mathrm{eff}} < 0$ and $Re(C_9^{\mathrm{eff}}) > 0$ throughout the kinematic region. Hence, Eq. (23) is satisfied for a point s_0, where s_0 is the zero-crossing point. However, in the Z' model, due to the inclusion of the NP couplings, $\mathrm{Re}(C_9^{NP}) < 0$ for the entire kinematic range. Since both $C_7^{\mathrm{eff}} < 0$ and $\mathrm{Re}(C_9^{NP}) < 0$, we do not obtain any point for $\hat{s}$ where Eq. (23) is satisfied in the Z' model. This indicates that $B \to \omega\mu^+\mu^-$ decay is sensitive to the effects of the Z' boson. Furthermore, the magnitude of the integrated value of forward-backward asymmetry is considerably higher than the SM value.

The longitudinal lepton polarization asymmetry, P_L, has also deviated from the SM prediction [Fig. 3(c)]. In the low-$\hat{s}$ region, the values of P_L in the Z' model are lower than those in the SM plot. However, in the high-$\hat{s}$ region, the Z' plot increases compared to the SM plot. In addition, in both the $\hat{s}$ bins as well as in the full kinematic region, the averaged values in the Z' model have deviated significantly from their corresponding SM values.

For the normal polarization asymmetry, the Z' plot has deviated significantly from the SM plot [Fig. 3(d)]. Even though the magnitudes of P_N for both the SM and Z' model are very small ($\sim 10^{-4}$ and $\sim 10^{-2}$), NP sensitivity is still depicted here, especially in the low-$\hat{s}$ region.

The variation of transverse polarization asymmetry in the SM and in Z' model is shown in Fig. 3(e). For the full $\hat{s}$ region, the Z' plot almost coincides with the SM plot. Hence, P_T is not as sensitive as the other observables are to the NP effects of the Z' boson. Nevertheless, the averaged value of P_T in the bin [0.039, 0.215] as well as the averaged value in the complete $\hat{s}$ range are higher in comparison to the SM value, signifying slight sensitivity to the Z' boson.

TABLE VIII. Binned values of the observables.

Observable	$\hat{s}$	SM	Z' model
Branching ratio	[0.003, 0.035]	$2.02^{+0.23}_{-0.24} \times 10^{-9}$	$2.44^{+0.23}_{-0.24} \times 10^{-9}$
	[0.039, 0.215]	$4.84^{+0.96}_{-0.94} \times 10^{-9}$	$6.59^{+0.94}_{-0.92} \times 10^{-9}$
Forward-backward asymmetry	[0.003, 0.035]	$0.102^{+0.009}_{-0.007}$	$-0.091^{+0.005}_{-0.006}$
	[0.039, 0.215]	$-0.012^{+0.002}_{-0.003}$	$-0.320^{+0.031}_{-0.040}$
Longitudinal lepton polarization asymmetry P_L	[0.003, 0.035]	$-0.142^{+0.066}_{-0.055}$	$-0.313^{+0.031}_{-0.026}$
	[0.039, 0.215]	$-0.740^{+0.047}_{-0.033}$	$-0.867^{+0.002}_{-0.001}$
Normal lepton polarization asymmetry P_N	[0.003, 0.035]	$1.002^{+0.091}_{-0.076} \times 10^{-4}$	$1.657^{+0.108}_{-0.092} \times 10^{-2}$
	[0.039, 0.215]	$3.923^{+0.785}_{-0.558} \times 10^{-4}$	$1.045^{+0.127}_{-0.100} \times 10^{-2}$
Transverse lepton polarization asymmetry P_T	[0.003, 0.035]	$0.413^{+0.005}_{-0.004}$	$0.396^{+0.005}_{-0.004}$
	[0.039, 0.215]	$0.106^{+0.005}_{-0.007}$	$0.108^{+0.002}_{-0.002}$

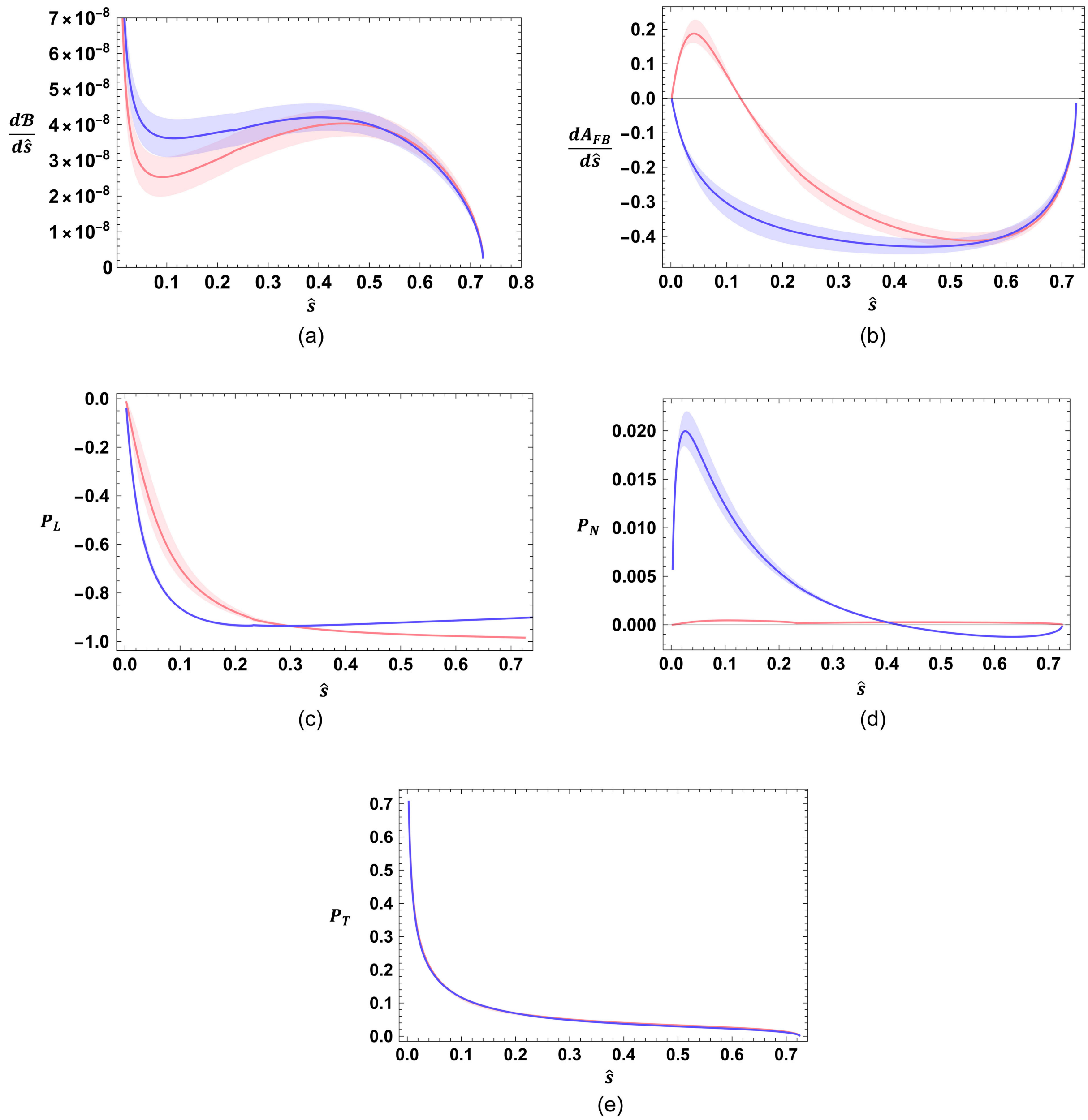

FIG. 3. The variation of the observables in the allowed kinematic region for (a) differential branching fraction, (b) forward-backward asymmetry, (c) longitudinal polarization asymmetry P_L, (d) normal polarization asymmetry P_N, and (e) transverse polarization asymmetry P_T. The pink line denotes the variation of the observable in the SM, while the blue line denotes the variation of the observable in the Z' model. The shaded regions in each plot correspond to the 1σ uncertainties which arise from the form factors.

VI. CONCLUSION

FCNC transitions in the B meson decay channels provide plenty of opportunities to investigate possibilities of NP signatures. In this work, we have explored $B \to \omega\mu^+\mu^-$ decay in the framework of the nonuniversal Z' model and evaluated several key observables of this decay channel. We have constrained the available parameter space of the NP leptonic coupling from other decays following $b \to d\ell^+\ell^-$ transition, while the NP quark coupling is constrained from UTfit Collaboration data for $B_d - \overline{B_d}$ mixing. These couplings were then incorporated in the modified Wilson coefficients in order to estimate observables in the Z' model. We have observed that the central value of the branching fraction in the available $\hat{s}$ range deviates from the SM prediction, mainly in the low- and mid-$\hat{s}$ region. In addition, our results also depict considerable deviation of forward-backward asymmetry from the SM result. In fact, the disappearance of the zero-crossing point of the forward-backward asymmetry in the nonuniversal Z' model suggests that this decay channel is highly sensitive to the NP effects of the Z' boson. Although the transverse

TABLE IX. Input parameters.

Parameter	Value [74]
m_μ	105.658 MeV
m_b	4.183 GeV
m_c	1.2730 GeV
M_{B^+}	5.27941 GeV
M_{B^0}	5.27963 GeV
M_{B_s}	5.36691 GeV
M_ω	0.78266 GeV
M_{π^+}	0.13957039 GeV
M_ρ	0.77526 GeV
M_{K^*}	0.895 GeV
M_W	80.3692 GeV
τ_{B^+}	1.638×10^{-12} s
τ_{B^0}	1.517×10^{-12} s
τ_{B_s}	1.516×10^{-12} s

polarization asymmetry does not differ much from the SM result, the longitudinal and the normal polarization asymmetries shift considerably from the corresponding SM plot. In addition, we have also calculated the values of the observables in two $\hat{s}$ bins. The values in both the bins for all the observables have deviated considerably from the SM calculations. The integrated values of the observables for the whole $\hat{s}$ region also have shifted from the SM values. Our results demonstrate that this decay mode provides a complementary and sensitive testing ground for detecting possible effects of NP beyond the SM.

ACKNOWLEDGMENTS

The authors thank the reviewer for the valuable comments and suggestions. M. M. acknowledges the Department of Science and Technology, Government of India, for providing the INSPIRE Fellowship through IF 200277. The authors also thank Dr. Swagata Biswas, Dr. Supravat Mahata, Mr. Hrushikesha Mahapatra, and Mr. Raja Ray for helpful discussions.

DATA AVAILABILITY

The data are not publicly available. The data are available from the authors upon reasonable request.

[1] S. L. Glashow, J. Iliopoulos, and L. Maiani, Weak interactions with lepton-hadron symmetry, Phys. Rev. D **2**, 1285 (1970).

[2] A. Ali, P. Ball, L. T. Handoko, and G. Hiller, A comparative study of the $B \to (K, K^*)\ell^+\ell^-$ decays in standard model and supersymmetric theories, Phys. Rev. D **61**, 074024 (2000).

[3] N. Cabibbo, Unitary symmetry and leptonic decays, Phys. Rev. Lett. **10**, 531 (1963).

[4] M. Kobayashi and K. Maskawa, *CP*-violation in the renormalizable theory of weak interaction, Prog. Theor. Phys. **49**, 652 (1973).

[5] W. G. Parrott, C. Bouchard, and C. T. H. Davies, Standard model predictions for $B \to K\ell^+\ell^-$, $B \to K\ell_1^-\ell_2^+$ and $B \to K\nu\bar{\nu}$ using form factors from $N_f = 2 + 1 + 1$ lattice QCD, Phys. Rev. D **107**, 014511 (2023).

[6] R. Aaij *et al.* (LHCb Collaboration), Differential branching fractions and isospin asymmetries of $B \to K^{(*)}\mu^+\mu^-$ decays, J. High Energy Phys. 06 (2014) 133.

[7] R. Aaij *et al.*. (LHCb Collaboration), Branching fraction measurements of the rare $B_s^0 \to \phi\mu^+\mu^-$ and $B_s^0 \to f_2'\mu^+\mu^-$ decays, Phys. Rev. Lett. **127**, 151801 (2021).

[8] R. Aaij *et al.* (LHCb Collaboration), Measurement of form-factor independent observables in the decay $B^0 \to K^{*0}\mu^+\mu^-$, Phys. Rev. Lett. **111**, 191801 (2013).

[9] R. Aaij *et al.* (LHCb Collaboration), Angular analysis of the $B^0 \to K^*\mu^+\mu^-$ decay using 3 fb^{-1} of integrated luminosity, J. High Energy Phys. 02 (2016) 104.

[10] I. Adachi *et al.* (Belle, Belle II Collaborations), Search for rare $b \to dl^+l^-$ transitions at Belle, Phys. Rev. Lett. **133**, 101804 (2024).

[11] A. Biswas, S. Nandi, S. K. Patra, and I. Ray, Study of the $b \to dll$ transition in the SM and test of NP, J. High Energy Phys. 03 (2023) 247.

[12] P. Nayek, P. Maji, and S. Sahoo, Study of semileptonic decays $B \to \pi l^+l^-$ and $B \to \rho l^+l^-$ in non-universal Z' model, Phys. Rev. D **99**, 013005 (2019).

[13] N. Farooq, M. Zaki, M. A. Paracha, and F. M. Bhutta, Effects of family non-universal Z' model in the angular observables of $B \to (\rho, a_1)\mu^+\mu^-$ decays, Chin. Phys. C **48**, 103107 (2024).

[14] A. K. Alok, A. Dighe, S. Gangal, and D. Kumar, Predictions for $B_s \to \bar{K}^*\ell\ell$ in non-universal Z' models, Eur. Phys. J. C **80**, 682 (2020).

[15] T. M. Aliev and M. Savci, Exclusive $B \to \pi\ell^+\ell^-$ and $B \to \rho\ell^+\ell^-$ in two Higgs doublet model, Phys. Rev. D **60**, 014005 (1999).

[16] Z. Aarfi, Q. M. U. Salam, I. Ahmed, F. M. Bhutta, R. Khalid, and M. A. Paracha, Investigating new physics through the observables of semileptonic $B_s \to K^*(\to K\pi)\mu^+\mu^-$ decay, Prog. Theor. Exp. Phys. **2025**, 123 (2025).

[17] R. Bause, H. Gisbert, M. Golz, and G. Hiller, Model-independent analysis of $b \to d$ processes, Eur. Phys. J. C **83**, 419 (2023).

[18] N. R. Soni, A. Issadykov, A. N. Gadaria, J. J. Patel, and J. N. Pandya, Rare $b \to d$ decays in covariant confined quark model, Eur. Phys. J. A **58**, 39 (2022).

[19] D. Bečirević, F. Jaffredo, J. P. Pinheiro, and O. Sumensari, Lepton flavor violation in exclusive $b \to d l_i l_j$ and $b \to s l_i l_j$ decay modes, Phys. Rev. D **110**, 075004 (2024).

[20] A. M. Marshall, M. A. McCann, M. Patel, K. A. Petridis, M. Reboud, and D. v. Dyk, Maximising the physics potential of $B^\pm \to \pi^\pm \mu^+ \mu^-$ decays, Phys. Rev. D **109**, 116013 (2024).

[21] A. V. Rusov, Probing new physics in $b \to d$ transitions, J. High Energy Phys. 07 (2020) 158.

[22] Q. Chang and Y. D. Yang, The effects of a family non-universal Z' boson in the $\bar{B}_s \to \pi K, \pi K^*$, ρK decays and $B_d - \bar{B}_d$ mixing, Nucl. Phys. **B852**, 539 (2011).

[23] S. Mahata, Study of B and D meson decays in beyond standard model, Doctoral thesis, National Institute of Technology Durgapur (2025), http://hdl.handle.net/10603/701955.

[24] J. J. Wang, R. M. Wang, Y. G. Xu, and Y. D. Yang, The rare decays $B_u^+ \to \pi^+ l^+ l^-, \rho^+ l^+ l^-$ and $B_d^0 \to l^+ l^-$ in the R-parity violating supersymmetry, Phys. Rev. D **77**, 014017 (2008).

[25] H.-Z. Song, L.-X. Lu, and G.-R. Lu, New physics effects on rare decays $B_u^+ \to \pi^+ \ell^+ \ell^-, \rho^+ \ell^+ \ell^-$ in a top quark two-Higgs-doublet model, Commun. Theor. Phys. **50**, 696 (2008).

[26] W.-F. Wang and Z.-J. Xiao, Semileptonic decays $B/Bs \to (\pi, k)(l^+ l^-, l\nu, \nu\bar{\nu})$ in the perturbative QCD approach beyond the leading order, Phys. Rev. D **86**, 114025 (2012).

[27] R. Aaij *et al.* (LHCb Collaboration), First observation of the decay $B^+ \to \pi^+ \mu^+ \mu^-$, J. High Energy Phys. 12 (2012) 125.

[28] R. Aaij *et al.* (LHCb Collaboration), First measurement of the differential branching fraction and CP asymmetry of the $B^\pm \to \pi^\pm \mu^+ \mu^-$ decay, J. High Energy Phys. 10 (2015) 034.

[29] J. P. Lees *et al.* (*BABAR* Collaboration), Search for the rare decays $B \to \pi \ell^+ \ell^-$ and $B^0 \to \eta \ell^+ \ell^-$, Phys. Rev. D **88**, 032012 (2013).

[30] R. Aaij *et al.* (LHCb Collaboration), Study of the rare B_s^0 and B^0 decays into the $\pi^+ \pi^- \mu^+ \mu^-$ final state, Phys. Lett. B **743**, 46 (2015).

[31] A. J. Buras and M. Munz, Effective Hamiltonian for $B \to X_s e^+ e^-$ beyond leading logarithms in the naive dimensional regularization and 't Hooft–Veltman schemes, Phys. Rev. D **52**, 186 (1995).

[32] F. Krüger and L. M. Sehgal, CP violation in the decay $B \to X_d e^+ e^-$, Phys. Rev. D **55**, 2799 (1997).

[33] G. Buchalla, A. J. Buras, and M. E. Lautenbacher, Weak decays beyond leading logarithms, Rev. Mod. Phys. **68**, 1125 (1996).

[34] Y. L. Wu, M. Zhong, and Y. B. Zuo, $B_s, D_s \to \pi, K, \eta, \rho, K^*, \omega, \phi$ transition form factors and decay rates with extraction of the CKM parameters $|V_{ub}|$, $|V_{cs}|$, $|V_{cd}|$, Int. J. Mod. Phys. A **21**, 6125 (2006).

[35] A. Ali and G. Hiller, A theoretical reappraisal of branching ratios and CP asymmetries in the decays $B \to (X_d, X_s) l^+ l^-$ and determination of the CKM parameters, Eur. Phys. J. C **8**, 619 (1999).

[36] M. Bauer, B. Stech, and M. Wirbel, Exclusive non-leptonic decays of $D-$, D_s- and $B-$ mesons, Z. Phys. C **34**, 103 (1987).

[37] W. Y. Wang, Y. L. Wu, and M. Zhong, Heavy to light meson exclusive semileptonic decays in effective field theory of heavy quarks, Phys. Rev. D **67**, 014024 (2003).

[38] M. Zhong, Y. L. Wu, and W. Y. Wang, Exclusive -meson rare decays and general relations of form factors in effective field theory of heavy quarks, Int. J. Mod. Phys. A **18**, 1959 (2003).

[39] L. Lin-xia, Z. Guo-fang, W. Shuai-wei, and Z. Zhi-qing, The rare decay $B_c \to D_s^* \mu^+ \mu^-$ in a family non-universal Z' model, Commun. Theor. Phys. **59**, 187 (2013).

[40] Q.-S. Yan, C.-S. Huang, L Wei, and S.-H. Zhu, Exclusive semileptonic rare decays $B \to (K, K^*) \ell^+ \ell^-$ in supersymmetric theories, Phys. Rev. D **62**, 094023 (2000).

[41] Paul Langacker and Michael Plumacher, Flavor changing effects in theories with a heavy Z' boson with family non-universal couplings, Phys. Rev. D **62**, 013006 (2000).

[42] M. Cvetic and P. Langacker, Z' physics and supersymmetry in book perspectives in supersymmetry, Adv. Ser. Dir. High Energy Phys. **18**, 312 (1998).

[43] P. Langacker, in *Particles, Strings, and Cosmology (PASCOS 98)*, edited by P. Nath (World Scientific, Singapore, 1999), p. 587.

[44] M. Masip and A. Pomarol, Effects of standard model Kaluza-Klein excitations on electroweak observables, Phys. Rev. D **60**, 096005 (1999).

[45] E. Nardi, Z' new fermions and flavor changing processes, constraints on E_6 models from $\mu \to eee$, Phys. Rev. D **48**, 1240 (1993).

[46] J. Bernabeu, E. Nardi, and D. Tommasini, $\mu - e$ conversion in nuclei and Z' physics, Nucl. Phys. **B409**, 69 (1993).

[47] V. D. Barger, M. S. Berger, and R. J. Phillips, Quark singlets: Implications and constraints, Phys. Rev. D **52**, 1663 (1995).

[48] M. B. Popovic and E. H. Simmons, Weak-singlet fermions: Models and constraints, Phys. Rev. D **62**, 035002 (2000).

[49] T. G. Rizzo, Gauge kinetic mixing and leptophobic Z' in E_6 and $SO(10)$, Phys. Rev. D **59**, 015020 (1999).

[50] H. Mahapatra, S. Mahata, M. Mandal, R. Ray, S. Biswas, and S. Sahoo, Exploring new physics effects of Z' boson on rare charm baryon Λ_c decay, Int. J. Mod. Phys. A **40**, 2550096 (2025).

[51] S. Biswas, R. Ray, M. Mandal, S. Mahata, H. Mahapatra, and S. Sahoo, Impact of new physics on polarization asymmetries of $\Sigma_b \to \Sigma_l l^+ l^-$ decays in nonuniversal Z' model, Int. J. Mod. Phys. A **40**, 2450162 (2025).

[52] M. Mandal, S. Biswas, S. Mahata, and S. Sahoo, Searching for new physics in $c \to u$ transitions with nonuniversal Z' model, Int. J. Mod. Phys. A **39**, 2450063 (2024).

[53] Ying Li, Guo-Hua Zhao, Yan-Jun Sun, and Zhi-Tian Zou, Family non-universal Z' effects on $B_{d,s} \to K^{*0} \bar{K}^{*0}$ decays in perturbative QCD approach, Phys. Rev. D **106**, 093009 (2022).

[54] M. K. Mohapatra, L. Nayak, R. Dhamija, and A. Giri, Delving into the $B_s \to l l'$, $B_{(s)} \to (K^{(*)}, \phi, f_2', K_2^*) l l'$ processes, arXiv:2302.03209.

[55] M. K. Mohapatra, N. Rajeev, and R. Dutta, Combined analysis of $B_c \to D_s^* \mu^+ \mu^-$ and $B_c \to D_s^* \nu\bar{\nu}$ decays within Z' and leptoquark new physics models, Phys. Rev. D **105**, 115022 (2022).

[56] V. Barger, L. L. Everett, J. Jiang, P. Langacker, T. Liu, and C. E. M. Wagner, $b \to s$ transitions in family-dependent $U(1)'$ models, J. High Energy Phys. 12 (2009) 048.
[57] C-W Chiang, L. R. Hui, and L. C. Dian, Study of $B \to K^{(*)}\ell^+\ell^-$ decays in the family non-universal Z' models, Chin. Phys. C **36**, 14 (2012).
[58] A. Arhrib, K. Chung, C-W. Chiang, and T-C. Yuan, Single top-quark production in flavor-changing Z' models, Phys. Rev. D **73**, 075015 (2006).
[59] K. Cheung, C.-W. Chiang, N. G. Deshpande, and J. Jiang, Constraints on flavor-changing Z' models by B_s mixing, Z' production, and $B_s \to \mu^+\mu^-$, Phys. Lett. B **652**, 285 (2007).
[60] Q. Chang and Y.-H. Gao, Probe a family non-universal Z' boson effects in $\bar{B}_s \to \phi\mu^+\mu^-$ decay, Nucl. Phys. **B845**, 179 (2011).
[61] Y. Li, J. Hua, and K.-C. Yang, $B \to K_1 l^+ l^-$ decays in a family non-universal model Z', Eur. Phys. J. C **71**, 1775 (2011).
[62] H. Chen and H. Hatanaka, Nonuniversal Z' couplings in B decays, Phys. Rev. D **73**, 075003 (2006).
[63] C.-W. Chiang, N. G. Deshpande, and J. Jiang, Flavor changing effects in family nonuniversal Z' models, J. High Energy Phys. 08 (2006) 075.
[64] V. Barger, L. Everett, J. Jiang, P. Langacker, T. Liu, and C. E. M. Wagner, Family non-universal $U(1)'$ gauge symmetries and $b \to s$ transitions, Phys. Rev. D **80**, 055008 (2009).
[65] R. Mohanta and A. K. Giri, Explaining $B \to K\pi$ anomaly with nonuniversal Z' boson, Phys. Rev. D **79**, 057902 (2009).
[66] J. Hua, C. S. Kim, and Y. Li, Annihilation-type charmless radiative decays of B meson in non-universal Z*ι* model, Eur. Phys. J. C **69**, 139 (2010).
[67] Q. Chang, X. Q. Li, and Y. D. Yang, Family non-universal Z' effects on $\bar{B}_q - B_q$, $B \to X_s\mu^+\mu^-$ and $B_s \to \mu^+\mu^-$ decays, J. High Energy Phys. 02 (2010) 082.
[68] M. Bona *et al.*, New physics from flavour, in *Melbourne Neutrino Theory Workshop (Neutrino 08)* (2009), p. 6, arXiv:0906.0953.
[69] M. Bona *et al.* (UTfit Collaboration), First evidence of new physics in $b \leftrightarrow s$ transitions, PMC Phys. A **3**, 6 (2009).
[70] http://www.utfit.org/UTfit/ResultsSummer2025NP.
[71] A. J. Buras, Weak Hamiltonian, *CP*-violation and rare decays, in, *Les Houches Summer School in Theoretical Physics, Session 68: Probing the Standard Model of Particle Interactions* (1998), Vol. 6, pp. 281–539, arXiv:hep-ph/9806471.
[72] A. J. Buras, Flavor dynamics: *CP*-violation and rare decays, Subnuclear Series **38**, 200 (2002).
[73] Y. Aoki *et al.*, FLAG review 2024, Phys. Rev. D **113**, 014508 (2026).
[74] S. Navas *et al.* (Particle Data Group), The review of particle physics (2025), Phys. Rev. D **110**, 030001 (2024).
[75] http://utfit.org/UTfit/ResultsSummer2025SM.